DOI: 10.18462/iir. 10.18462/iir.icr.2023.XXXX

Evolutionary optimization of heat exchanger circuitries for the advancement of next-generation refrigerants

Niccolo GIANNETTI*[(a)], Adriano MILAZZO[(b)], John Carlo S. GARCIA[(c)], Richard Jayson VARELA[(c)], Yuichi SEI[(d)], Koji ENOKI[(e)], Kiyoshi SAITO[(c)]

[(a)] Waseda Institute for Advanced Study, Waseda University,
Tokyo 169-8050, Japan, niccolo@aoni.waseda.jp
[(b)] Department of Industrial Engineering, University of Florence,
Florence 50139, Italy, adriano.milazzo@unifi.it
[(c)] Department of Applied Mechanics and Aerospace Engineering, Waseda University,
Tokyo 169-8555, Japan, saito@waseda.jp
[(d)] Department of Informatics, The University of Electro-Communications,
Tokyo 182-8585, Japan, seiuny@uec.ac.jp
[(e)] Department of Mechanical and Intelligent Systems Engineering, The University of Electro-Communications, Tokyo 182-8585, Japan, enoki.koji@uec.ac.jp

*Corresponding author: niccolo@aoni.waseda.jp

ABSTRACT

This study presents an assessment technique based on the evolutionary optimization of heat exchanger circuitries for the performance evaluation of next-generation refrigerants. A novel evolutionary algorithm is developed to handle the implementation of genetic operators with unrestrained number and location of splitting and merging nodes, while ensuring the circuitry feasibility. The circuitry optimization is conducted for a finned-tube evaporator with 36 tubes under given cooling capacity, degree of superheat, and heat source boundary conditions representative of air conditioning applications. The thermodynamic interrelations between minimum entropy generation and maximum COP are discussed, identifying optimal configurations of the heat exchanger that maximize the performance of each refrigerant. It is shown that low-GWP zeotropic mixtures with temperature glide exhibit the largest benefit from the developed circuitry optimization procedure and may achieve performance comparable to R32 and higher than R410A by approaching a Lorenz cycle operation.
Keywords: Circuitry optimization, zeotropic mixtures, thermodynamic losses, Lorenz cycle

1. INTRODUCTION

In the path towards decarbonization of the HVAC-R field, stricter regulations have pushed the development of new low-GWP refrigerants blends. In this context, although we may say that there is no perfect refrigerant for satisfying multiple selection criteria and a large variety of application cases, mixtures have increased the degrees of freedom in the spectrum of available fluids and may more closely provide appropriate alternatives to conventional substances. However, the performance evaluation of these new low-GWP refrigerants remains inconclusive. For instance, although zeotropic mixtures are recognized as promising low-GWP alternatives with potential thermodynamic benefits coming from the possibility of realizing a Lorenz cycle operation, in practice, these advantages remain unexploited due to some unresolved issues. Among those, we may mention challenging transfer properties, such as larger pressure drop or lower transfer coefficient than conventional substances, and unavailability of effective optimization methodologies for maximising heat transfer and minimizing thermodynamic losses within heat exchangers. These issues preclude taking advantage of the characteristic temperature glide, which limits the effectiveness of the heat exchangers with unnecessary thermodynamic losses, and increase the required refrigerant-air mean temperature difference. Therefore, to investigate optimal refrigerant choices, we focus on the heat exchangers, as components that have critical influence on the overall system performance and represent the interface with specific application cases. The heat exchanger performance is the result of air-side heat transfer and two-phase refrigerant heat, mass, and momentum transfer. These transport phenomena exhibit different characteristics and intensity in relation to different refrigerant properties and structural characteristics of the heat exchanger, such as splitting and merging junctions, that locally define refrigerant flow rate and quality distribution. In fact, more efficient and compact heat exchangers may be obtained by acting on the refrigerant circuitry to optimize local thermal matching between air and refrigerant temperatures, pressure drop, and heat transfer coefficient in relation to the refrigerant characteristics for given system requirements. Accordingly, this work suggests that refrigerant circuitry optimization may be a cost-effective procedure for supporting the deployment of next-generation low-GWP refrigerants. Previous research has suggested the use of evolutionary search methods, such as Genetic Algorithm, to deal with the search space of possible tube-connections in a heat exchanger, which is too large to be managed with empirical approaches, but no conclusive optimization tool has been established due to two main challenges:

- unsuitable mathematical representations of the refrigerant circuitry, which yield non-bijective relations between physical circuitry and its mathematical representation, and are unable to detect infeasible circuitries;
- limited search spaces, where only simple circuits with predetermined location and number of splits are considered, required by ineffective evolutionary techniques unable to manage genetic operators on complex circuitries.

To overcome these issues, this study relies on concepts of graph theory to develop a suitable mathematical representation of the refrigerant circuitry, and uses Genetic Programming to apply genetic operators to an unrestrained search space of complex circuitries, where arbitrary location and number of splitting/merging junctions are investigated.

2. HEAT EXCHANGER SIMULATOR AND CIRCUITRY OPTIMIZATION TOOL

A finned-tube heat exchanger simulator is designed around a bijective mathematical representation of the refrigerant circuitry, called Tube-Tube Adjacency Matrix, and a formulation of the related constraints to ensure the coherence and feasibility of the circuitry during the evolutionary search. Consequently, a novel evolutionary algorithm for refrigerant circuitry optimization is developed.

2.1. Circuitry formulation

For investigating different refrigerant circuitries the "tube-tube adjacency matrix" was developed in a previous study (Garcia et al. ………), which is inspired by the concepts of graph theory. This approach ensures a one-to-one relationship between circuitry and corresponding mathematical representation (Fig. 1), and summarizes all the required information to set up energy and mass balance. Additionally, in combination with traversal algorithms such as breadth-first search and depth-first search, it facilitates the formulation of topology constraints to ensure the physicality and feasibility of circuitry during evolutionary searches.

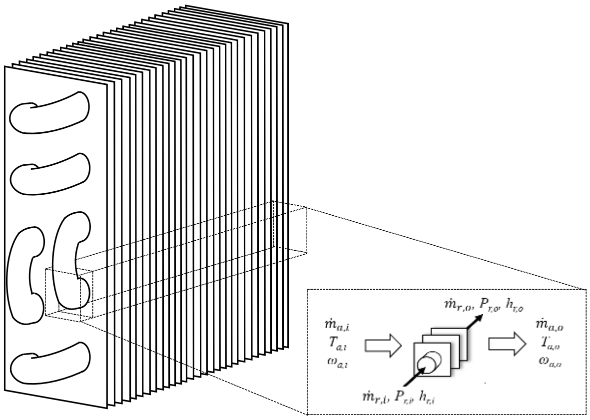

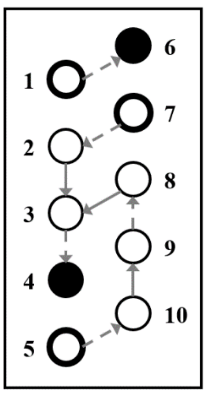

Reference	Connected tubes									
	1	2	3	4	5	6	7	8	9	10
1	0	0	0	0	0	1	0	0	0	0
2	0	0	1	0	0	0	-1	0	0	0
3	0	-1	0	1	0	0	0	-1	0	0
4	0	0	-1	0	0	0	0	0	0	0
5	0	0	0	0	0	0	0	0	0	1
6	-1	0	0	0	0	0	0	0	0	0
7	0	1	0	0	0	0	0	0	0	0
8	0	0	1	0	0	0	0	0	-1	0
9	0	0	0	0	0	0	0	1	0	-1
10	0	0	0	0	-1	0	0	0	1	0

Figure 1: Illustrations of a finned-tube heat exchanger and its corresponding tube-tube adjacency matrix

The management of the number and location of splits and merges in refrigerant circuitry optimization is motivated by the necessity of optimizing local temperature difference between air and refrigerant, and balance between air-side and refrigerant-side thermal resistances while limiting pressure drop. Accordingly, the direct application of genetic operators to the chromosome of the parent circuitries may results in infeasible and non-physical offspring. As a result, the generation of infeasible and nonphysical circuitries must be excluded based on the formulation of the following topology constraints. Five categories of infeasible and non-physical circuitry arrangements are considered (Fig. 2): I.) non-connected tubes, II.) infeasible internal loops, III.) upstream flows of a merge come from opposite sides of the heat exchanger, IV.) U-bends longer than a prescribed manufacturing limit, and V.) heat exchanger outlet flows at different sides. Limiting possible gene combinations using these constraints can significantly reduce the size of the search space and help the evolutionary algorithm converging toward optimal solutions. Mathematical details can be found in 26).

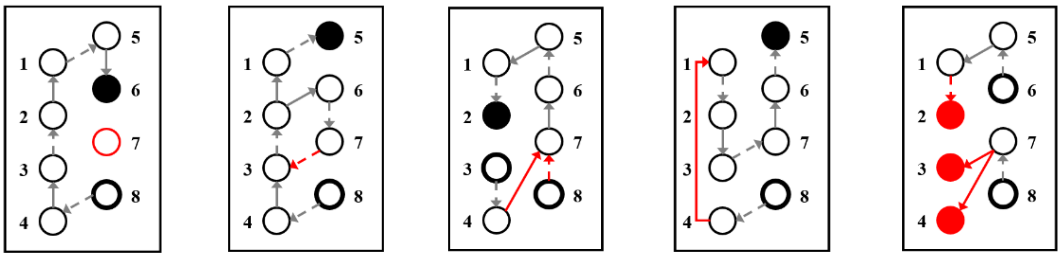

Figure 2: Feasibility and physicality constraints

2.2. Heat exchanger simulator

2.2.1. Numerical model

The model is developed while limiting calculation cost for effectively dealing with evolutionary search methods. A tube-by-tube approach is considered along with the assumptions of steady-state, negligible change in potential and kinetic energy, negligible heat transfer in the tube bends, and uniform air distribution. Heat transfer and pressure drop of the air are modelled with Kim-Youn-Webb (1999) and Kim-Youn-Webb (1999) correlations for airside heat transfer coefficient and pressure drop, respectively. Refrigerant-side heat transfer is modelled by using Shah correlations () and () for saturated boiling heat transfer of pure refrigerants and zeotropic mixtures, respectively, and Dittus-Boelter equation (…) for single-phase heat transfer coefficient. Muller-Steinhagen and Heck (1986) is adopted for two-phase refrigerant pressure gradient. In the return bends Popiel and Wojtkowiak (34) is used in calculating the single-phase pressure drop, while and Domanski and Hermes (35) for two-phase flow.

2.2.2. Experimental validation

The model was validated with dedicated experimental tests on a 28-tube evaporator using R410A (Fig 3).

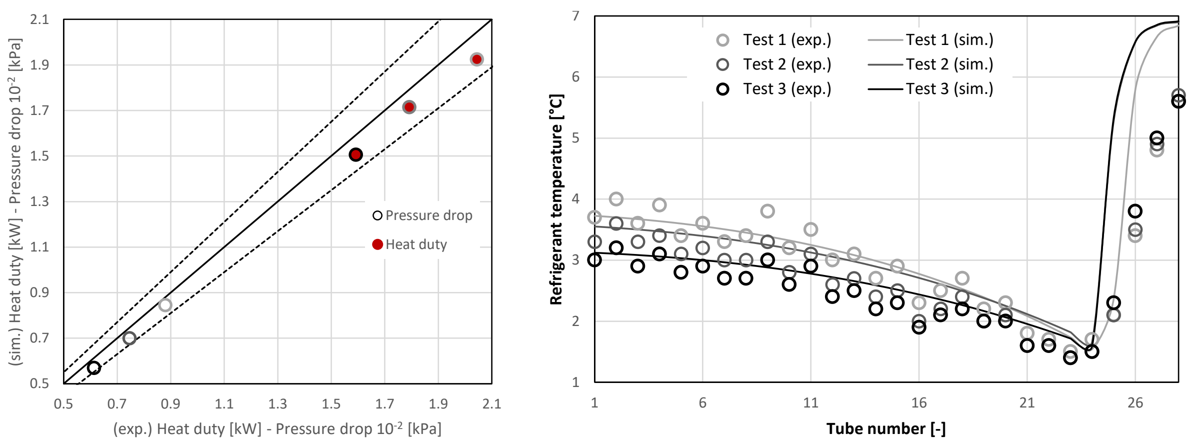

Figure 3: Experimental validation of total heat duty, total pressure drop, and local refrigerant temperature

It was found that the simulated overall heat duty and pressure drop were within 7 and 8% of the experimental values. Additionally, also the accuracy of the local temperature distribution was confirmed.

2.2.3. Entropy generation

Among other techniques, the assessment of irreversibility for the efficient design of heat exchangers has been generally recognized since the theoretical work of Bejan, complementarily expanded by Grazzini and Gori (1988), and extensively applied to technical optimization cases (). In this study, local air and refrigerant states are calculated as a result of the numerical model presented above. Accordingly, each tube's air-side and refrigerant-side entropy generation is calculated as in Eq. (1) and Eq. (2), respectively.

$$S_{gen,a} = \dot{Q}\,\frac{T_a - T_w}{T_a T_w} + \dot{m}_a \frac{v_a}{T_a} \Delta P_a \qquad \text{Eq. (1)}$$

$$S_{gen,r} = \dot{Q}\,\frac{T_w - T_r}{T_w T_r} + \dot{m}_r \frac{v_r}{T_r} \Delta P_r \qquad \text{Eq. (2)}$$

2.3. Circuitry optimization algorithm

Evolutionary algorithms have been widely used to solve optimization problems based on their robustness and flexibility for deriving solutions in complex spaces. Progression techniques inspired by Darwinian evolution are implemented, including selection, recombination, and mutation.

2.3.1. Genetic refrigerant path-algorithm

The developed "Genetic refrigerant path-algorithm" is a path generation algorithm based on the principles of genetic programming, which applies genetic operators to tree structures while overcoming previous research limitations in managing unrestricted numbers and locations of splits and merges. In such tree structures, each node corresponds to a unique tube and is generated according to rules designed to exclude infeasible circuitries. Each tree (circuit) starts with root nodes (inlet tubes) and ends with leaves (outlet tubes). A tree can branch into subtrees if there are splits and merges in a circuit. The depth of a tree is equal to the number of nodes that must be traversed to reach a leaf from the root node (Fig. 4).
The proposed algorithm consists of five main phases: I.) initialization, II.) selection, III.) crossover, IV.) mutation, and V.) application of physical constraints.

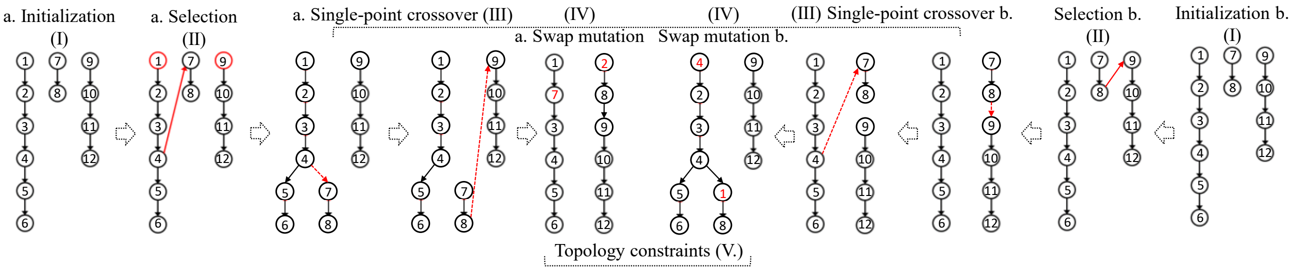

Figure 4: Illustration of the main phases of the path generation algorithm

The search process is based on a first initialization of the population and the evolution towards following generations. The population individuals from each generation are evaluated on the basis of a fitness function and the selection of parents is based on the roulette wheel method, where the probability of an individual to be chosen as a parent is proportional to its fitness value. Consequently, genetic operations such as crossover and mutation are applied to the parent circuitries to obtain new offspring circuitries. Finally, it is ensured that the resulting tree structures satisfy the physicality and feasibility constraints of actual refrigerant circuitries of heat exchangers and the generated structures are selected for the next generation. The process is repeated until convergence to the optimization criterion or until the maximum number of generations is reached.

2.3.2. Optimization settings

The proposed evolutionary algorithm is applied to an evaporator of an air conditioner cycle for evaluating the potential performance of different refrigerants for a given application case. The search for refrigerant circuitries yielding optimal results for a given objective function is performed under the following settings and constraints representing the requirements of the given application case. Calculations are conducted for a 36-tubes evaporator with 12 tube rows and features of the transfer surface previously adopted in Domanski (…) (Table 2). Additionally, input parameters, such as return room air temperature, and inlet enthalpy of the evaporator defined isenthalpically by condensing temperature and degree of subcooling, are as summarised in Table 1. Contextually, iterated values are the local refrigerant state and flowrate at each tube, in addition to the total refrigerant and air flow rates, and the inlet pressure to the evaporator while converging to given cooling capacity, supply air temperature, and degree of superheat requirements. Optimization runs adopt a population size of 500, times 100 generations, hence investigating 50,000 circuitries for each run.

Table 1. Operating and target conditions

Return air temperature	26 (°C)
Supply air temperature	18 (°C)
Degree of superheat	5 (K)
Cooling capacity	4,6,8,10 (kW)
Condensing temperature	45 (°C)
Degree of subcooling	5 (K)
Isentropic efficiency / Motor efficiency	0.85/0.85

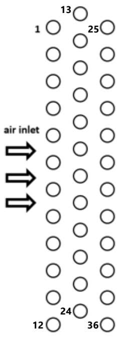

Table 2. Evaporator dimension and features

Tube outer diameter	0.01 (m)
Tube inner diameter	0.0092 (m)
Tube length	0.5 (m)
Tube longitudinal pitch	0.0222 (m)
Tube transverse pitch	0.0254 (m)
Fin spacing	0.002 (m)
Fin thickness	0.0002 (m)

2.3.3. Objective function

For given cooling capacity, the cycle COP may be maximised by minimising the compressor work. Under the calculation conditions listed in Table 1, maximum cycle efficiency may be approached by searching for circuitries able to maximise the outlet pressure of the evaporator (Eq. 3).

$$COP = \frac{\dot{Q}_e}{\dot{W}} = \frac{\dot{Q}_e}{\dot{m}\Delta h_{comp}} = \frac{\dot{Q}_e}{\dot{Q}_e/_{\Delta h_e \eta_{comp}} \; \Delta h_{is}/_{\eta_{comp}}} = \frac{1}{\frac{1}{\eta_{comp}} \frac{h(p_{cond}, s_{out,e}) - h(p_{out,e}, T_{sat}(p_{out,e}) + 5K)}{h(p_{out,e}, T_{sat}(p_{out,e}) + 5K) - h_{in,e}}} \qquad \text{Eq. (3)}$$

Contextually, the outlet pressure of the evaporator may be maximised by reducing pressure drop and mean temperature difference between refrigerant and air. The following numerical investigation is motivated by the observation that for reducing pressure drop and mean temperature difference it is necessary to minimize the corresponding irreversible thermodynamic losses, namely the entropy generation arising from friction and entropy generation related to finite-temperature-difference heat transfer. Accordingly, the objective function adopted to evaluate the fitness of the circuitries generated with the genetic refrigerant path-algorithm is the minimum total entropy generation defined as in Eq. (4). The corresponding optimization results are discussed to investigate the ability of the proposed optimization method to define suitable features of the refrigerant circuitry for different refrigerants and given operation requirements. Contingently, thermodynamic interrelations between minimum entropy generation and maximum COP are discussed.

$$S_{gen} = \sum_{n=1}^{N_{tubes}} \left(\dot{Q}\,\frac{T_w - T_r}{T_w T_r} + \dot{Q}\,\frac{T_a - T_w}{T_a T_w} + \dot{m}_r \frac{v_r}{T_r} \Delta P_r + \dot{m}_a \frac{v_a}{T_a} \Delta P_a \right)_n \qquad \text{Eq. (4)}$$

3. RESULTS AND DISCUSSION

Three representative refrigerants for air conditioning applications are investigated: a pure refrigerant (R32), a near–azeotropic mixture (R410A), and an alternative low-GWP zeotropic mixture (R454C).

Figure 5 exemplifies the evolutionary progression of the search algorithm under the conditions described above for the optimization run conducted with R32 refrigerant, under the cooling capacity requirement of 6 kW. Although Lee et al. (2016) concluded that entropy generation minimization is an unsuitable method for the analysis of optimal refrigerant circuitries because of an often-dominant effect of heat transfer over friction irreversibility, this study demonstrates the consistency between minimum entropy generation and maximum COP when calculations settings require convergence to a given output capacity requirement. Specifically, Fig. 5 shows that, under the calculation conditions defined by Table 1, when heat transfer irreversibility can be lowered at the expenses of a moderately larger pressure drop, the total entropy generation at the corresponding evaporator may be reduced and the cycle COP improved.

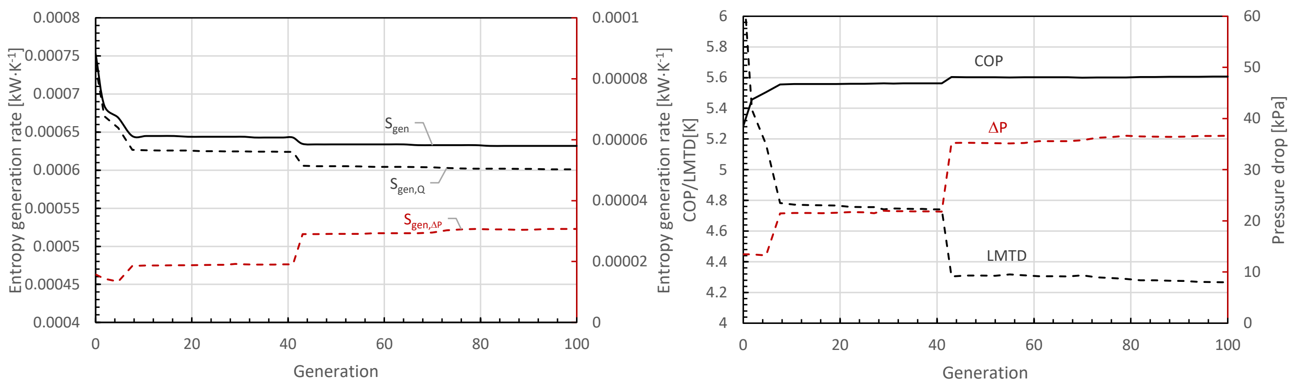

Figure 5: Evolutionary minimization of entropy generation and corresponding progression of COP, ΔP, and LMTD

The optimization runs are conducted for each refrigerant and each required cooling capacity. A near-optimum circuitry is returned as a result of each run. Figure 6 shows the resulting circuitries for R32. In these schematics, the inlet tubes are represented by thick-bordered circles, outlet tubes by "O" symbols, and splits by "S" symbols. The solid lines represent the return bends on the front side of the heat exchanger, whereas the return bends on the back side are represented by dashed lines.

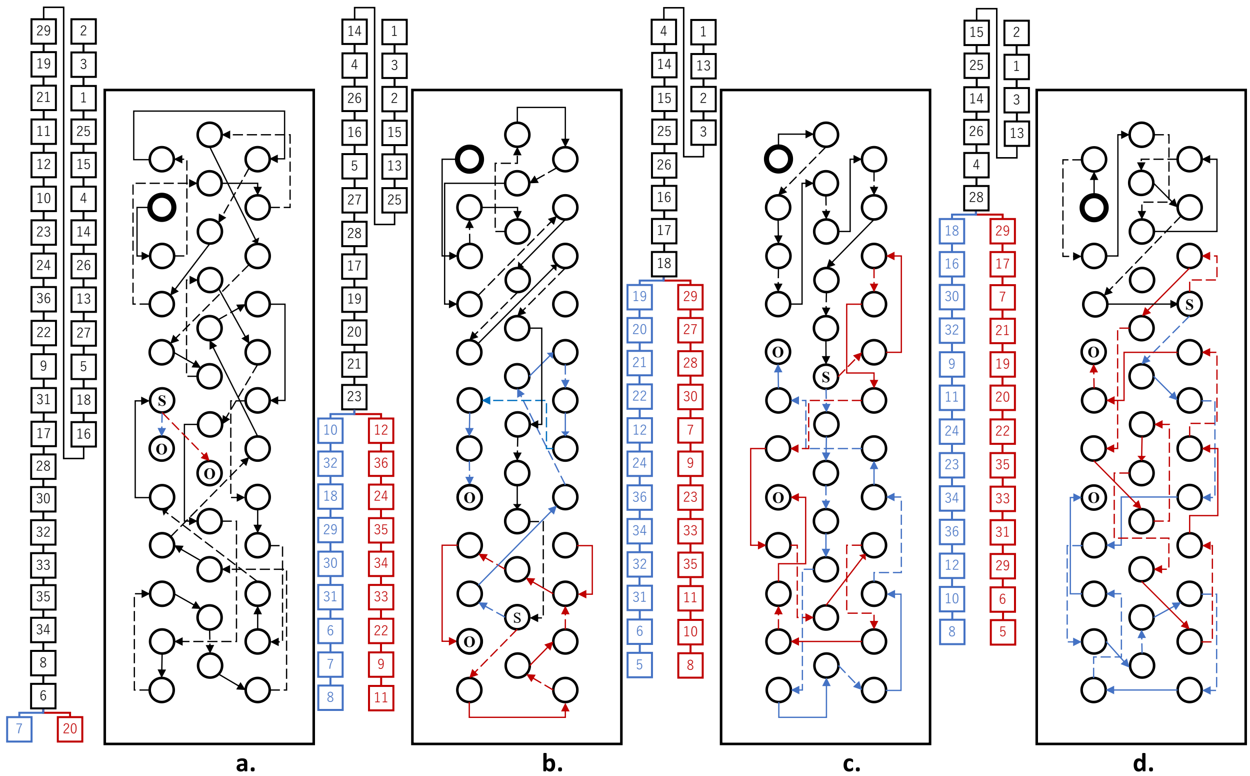

Figure 6: Optimized refrigerant circuitries for R32; (a) 4 kW, (b) 6 kW, (c) 8 kW, (d) 10 kW

One can see that the number of circuits and split location vary with the refrigerant and target capacity. Specifically, as the capacity increases for a given refrigerant, the location of the split moves ahead to limit the refrigerant pressure drop by reducing the local refrigerant flow rate. Additionally, the latent heat of vaporization affects the flow rate required to achieve the target cooling capacity. Based on its large latent heat, among the three refrigerants, R32 requires the lowest refrigerant flow rate to achieve the target capacity, whereas R454C requires the highest flow rate.

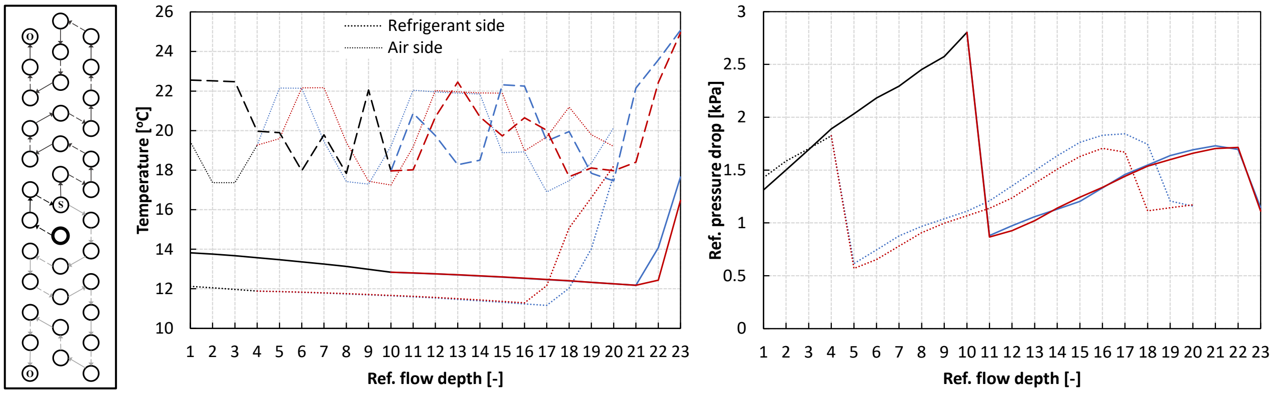

Figure 7: Local refrigerant pressure drop and refrigerant / air temperatures for R32 and 10-kW cooling capacity

Additionally, the refrigerant circuitry determines the distribution of the local temperature difference between the air and refrigerant, which could be optimized to reduce irreversible heat transfer losses related to the refrigerant saturation temperature variation caused by the pressure drop and temperature glide of zeotropic mixtures.

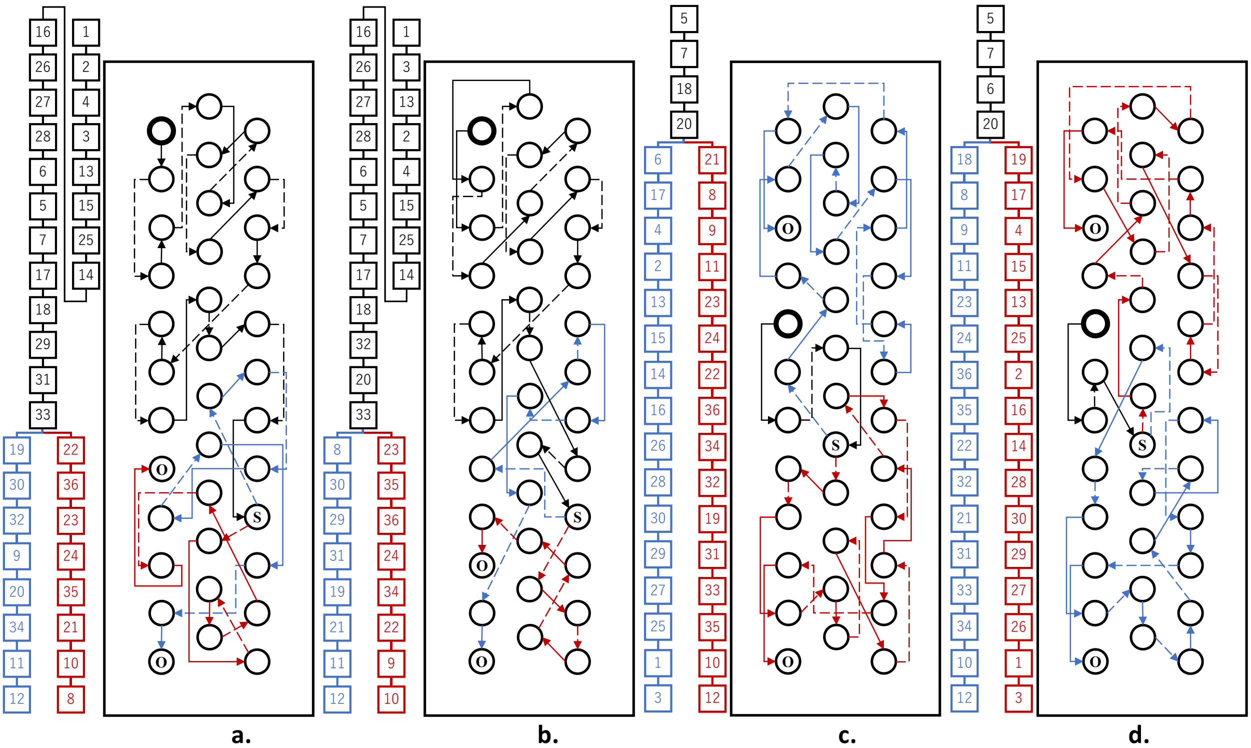

Figure 8: Optimized refrigerant circuitries for R410A; (a) 4 kW, (b) 6 kW, (c) 8 kW, (d) 10 kW

Figure 7 illustrates the local refrigerant pressure drop as well as refrigerant and air temperatures along the refrigerant flow for the case of R32 and a 10-kW cooling capacity. The horizontal axis in represents the depth of the refrigerant flow (in no. of tubes) in each branch of the circuitry. The air temperature (dashed line) is arranged according to the refrigerant path in order to highlight the local temperature difference between the air and refrigerant, hence, not representing the continuity of the air flow. Results representing a representative baseline serpentine (thin dotted lines) and the optimized circuitries (thicker continuous and dashed lines). Contextually, a notable feature of the optimized circuitries compared to the baseline is the presence of fewer tubes in the superheated refrigerant state. This improves the usage of the transfer surface by minimizing the part of the transfer area that interfaces with a low heat transfer coefficient on the refrigerant side. Consequently, the optimized circuit can achieve the same capacity while maintaining a smaller temperature difference between the refrigerant and air throughout the heat exchanger.

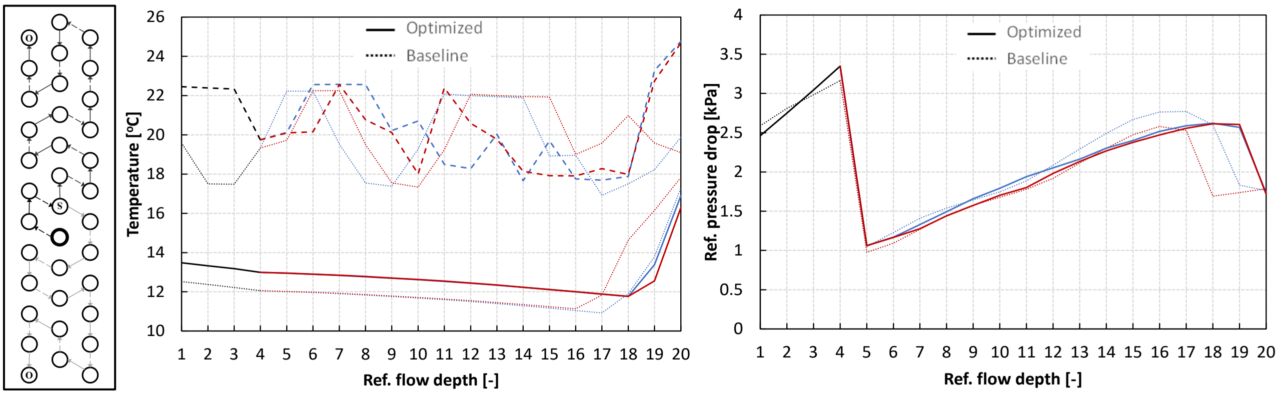

Figure 9: Local refrigerant pressure drop and refrigerant / air temperatures for R410A and 10-kW cooling capacity

Corresponding observations apply to the results obtained for the near-azeotropic mixture R410A both for the optimized circuitries (Fig. 10) and the effect on local temperature and pressure drop distributions (Fig. 11). The optimized circuitries operate at a higher inlet evaporator pressure because the split location moves closer to the outlet, which results in locally higher pressure drop (Figs. 9-11), but also in a larger heat transfer coefficient. Additionally, the rearrangement of the tubes ordering improves the local distribution of the temperature difference between the air and refrigerant.

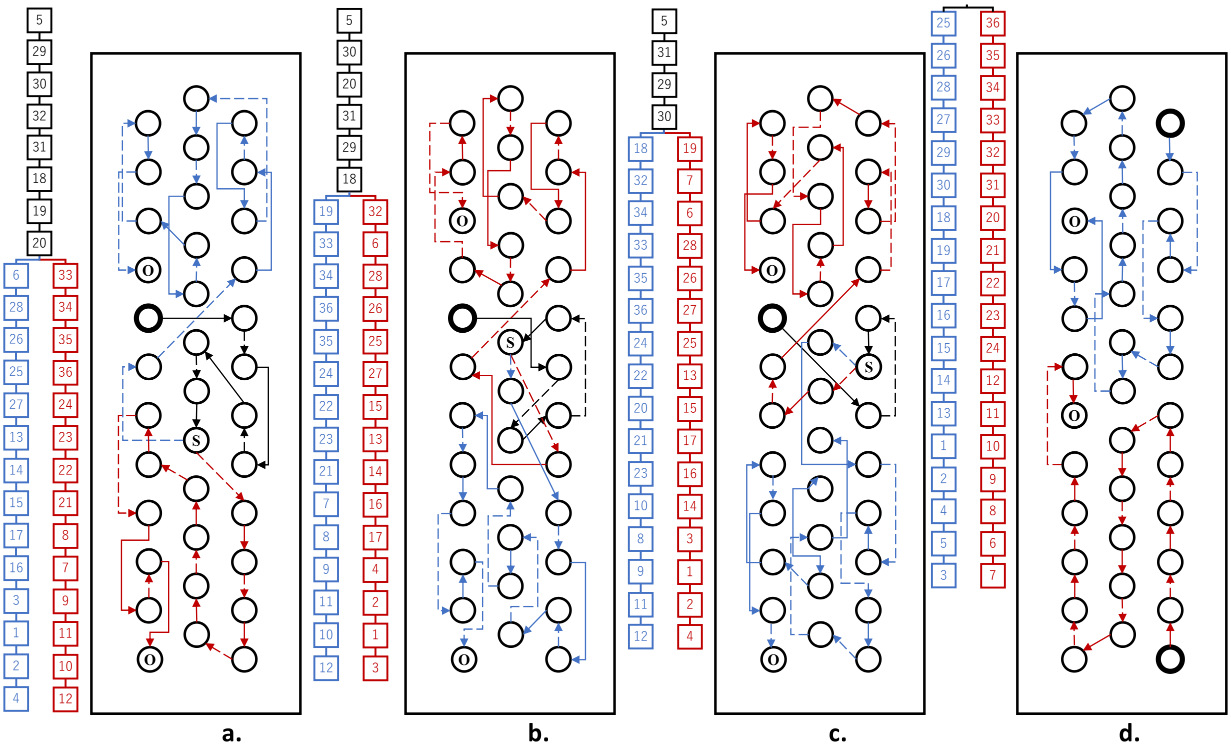

Figure 10: Optimized refrigerant circuitries for R454C; (a) 4 kW, (b) 6 kW, (c) 8 kW, (d) 10 kW

A different trend can be observed in the R454C evaporators because of the large temperature glide and different thermophysical and transport properties of the zeotropic mixture. Figure 10 presents the resulting optimized circuitries for R454C, while Fig. 11 illustrates the local refrigerant temperature distribution and pressure drop of the baseline and optimized circuitries for a required 10-kW capacity. The optimized R454C circuitry operates at a lower evaporator inlet pressure, but a higher outlet pressure, than the baseline circuitry, which deviates from the general trend of the optimization results. This characteristic is a result of having two parallel circuits and featuring correspondingly lower pressure drop.

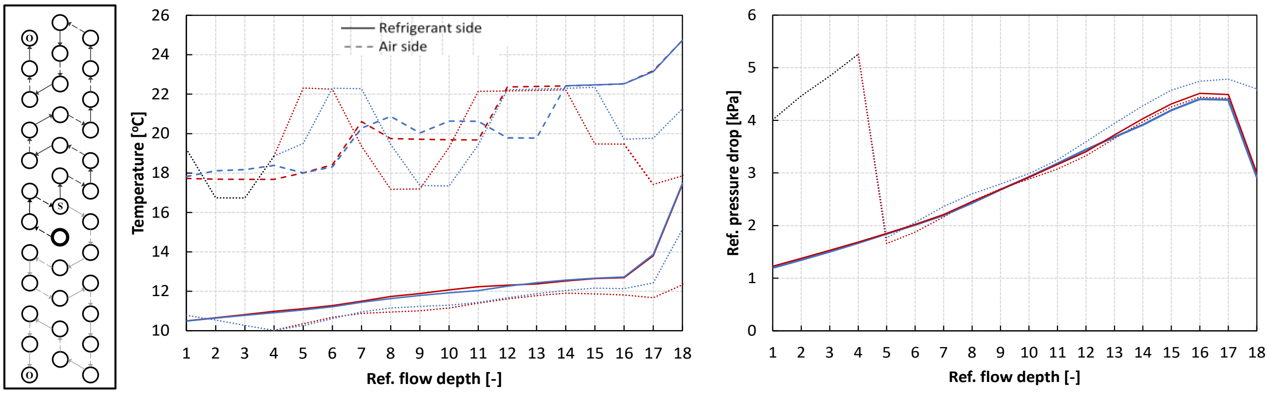

Figure 11: Local refrigerant pressure drop and refrigerant / air temperatures for R454C and 10-kW cooling capacity

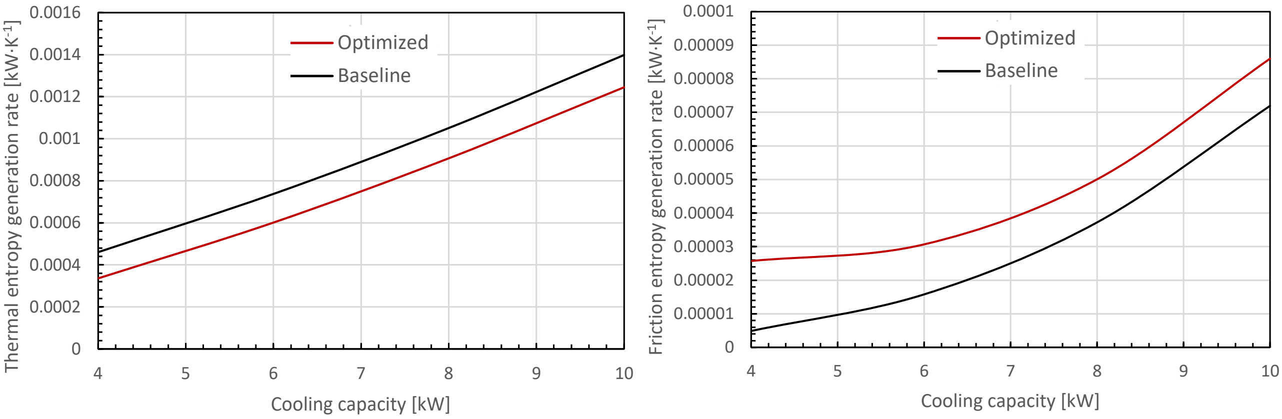

Figure 12: Thermal and friction entropy generation vs cooling capacity of optimized and baseline circuitries for R32

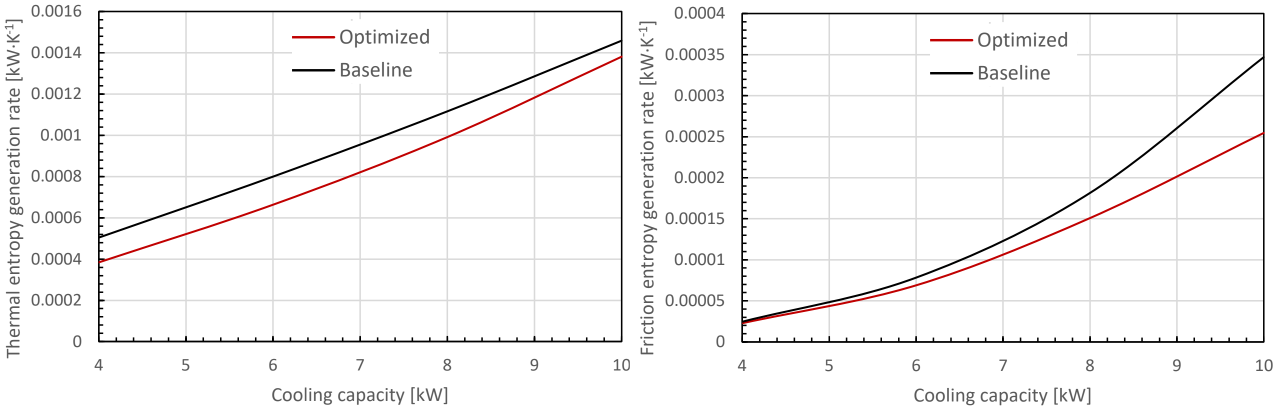

Figure 13: Thermal and friction entropy generation vs cooling capacity of optimized and baseline circuitries for R454C

As shown in Fig. 11, the temperature glide cannot be effectively utilized if large pressure drops are encountered on the refrigerant side. The temperature of R454C in the baseline circuitry decreases before the split as a result of pressure drop. Therefore, the optimized circuitry can take advantage of R454C's temperature glide by maintaining low values of pressure drop and maximizing the effects of a counter-flow arrangement between the air and refrigerant flows.

Figures 12 and 13 globally represent the concepts discussed above by showing that optimized circuitries for azeotropic refrigerants are achieved by reducing the thermal entropy generation and increasing friction entropy generation over the whole investigated range of cooling capacity, whilst for zeotropic refrigerants both thermal and friction entropy generation rates are lowered, especially at high cooling capacity.

As demonstrated in Fig. 14, following circuitry optimization by minimizing entropy generation, R454C demonstrated higher COP than R410A and may achieve performance comparable to R32 at 4 kW capacity. The optimization approach was able to indicate a refrigerant path that utilized the temperature glide of R454C and determine the appropriate number of circuits that minimized the pressure drop and finite-temperature-difference heat transfer between air and refrigerant for given target cooling capacity, superheat at the compressor suction, and temperature level of external environment and indoor space. The reasons for a larger improvement achieved for zeotropic refrigerant mixtures is to be ascribed to the possibility, in these cases, to approach a Lorenz-cycle operation for the same temperature levels of indoor and outdoor heat sources and sinks.

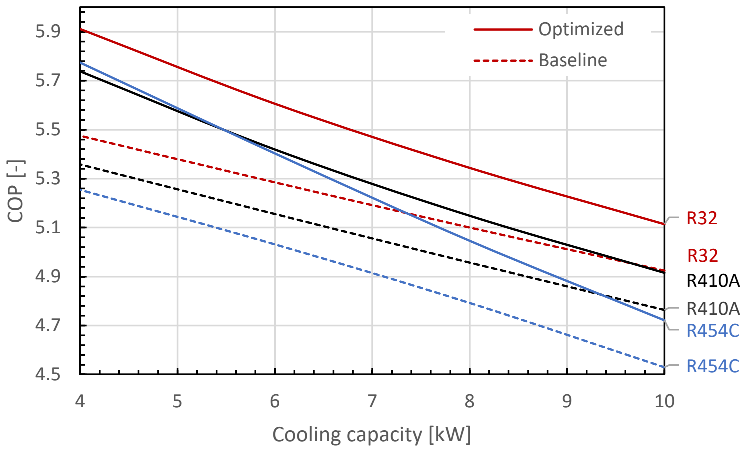

Figure 14: Comparison of resulting COP calculated with optimized and baseline circuitries for different refrigerants

4. CONCLUSIONS

A new evolutionary method for the optimization of heat exchanger circuitry was proposed and tested for the thermodynamic optimization of a 36-tube evaporator in representative conditions of air conditioning applications. The performance of R32, R410A, and R454C is correspondingly assessed after minimizing entropy generation under given heat source and sink boundary conditions, degree of superheat, and output capacity. When calculations settings are accordingly defined, this study demonstrates the consistency between minimum entropy generation and maximum COP. The implementation of the new circuitry optimization algorithm finds efficient heat exchanger topologies by minimizing pressure drop, mean average temperature difference between the refrigerant and the air side, and the number of ineffective tubes in a superheated state. As a result, the evaporator outlet pressure was increased, the compression ratio was reduced, and the COP was maximised under the given optimisation constraints.

The use of this optimisation technique is proposed for assessing the performance of next-generation zeotropic refrigerant mixtures. The combination of these new methods enables the search for optimal topologies of heat exchangers in a way that makes possible to take advantage of the thermodynamic benefits of non-azeotropic refrigerants by approaching the Lorentz cycle operation. The results demonstrate that non-azeotropic refrigerant mixtures with low-GWP may exhibit higher performance than R410A and comparable to R32.

ACKNOWLEDGEMENTS

This paper is based on results obtained from a project commissioned by the New Energy and Industrial Technology Development Organization (NEDO).

NOMENCLATURE

p	pressure (kPa)	R	molar gas constant (8.314472 J×mol^{-1}×K^{-1})
T	temperature (K)	V	molar volume (m^3×mol^{-1})

REFERENCES

The sources should be presented as follows:

Journal paper: Name(s) of the author(s), first name initial(s)., year of publication. Title of article. Journal title. Volume number, issue number (between parenthesis), Page range of article.

Article from a periodical: Name(s) of the author(s), first name initial(s)., year of publication. Title of article. Title of periodical and abbreviated according to international standards, Volume number, issue number (between parenthesis), Page range of article.

Paper published in conference proceedings: Name(s) of the author(s), first name initial(s)., year of publication. Title of article. Title of the conference, publisher of proceedings, Page range of article.

Book: Name(s) of the author(s), first name initial(s)., year of publication. Title of the book. Name of publisher, place of publication, number of pages. Establishments can be considered authors when they assume main responsibility for the text and their publications reflect their collective reflections or activities.

Book chapter: Name(s) of the author(s), first name initial(s)., year of publication. Title of chapter. In: name(s) and initial(s) of the co-ordinator(s), title of the book, name of publisher, place of publication, Page range of article.

For instance:

Duminil, M., 1995. Principes de la production du froid. In: Côme, D., Ulrich, R., La chaîne du froid – Le froid au service de l'homme, Hermann, Paris, 33-144.

Herbe, L., Lundqvist, P., 1997. CFC and HCFC refrigerants retrofits. Int. J. Refrigeration 20(1), 49-54.

Janna, S.W., 1986. Engineering Heat Transfer. PWS Publishers, Boston, 769 p.

Pearson, S.F., 1996. Uses of Hydrocarbon Refrigerants. Proceedings of the IIR Conference on Applications for Natural Refrigerants, Aarhus, Denmark, IIF/IIR, 439-446.